Journal of Materials Chemistry A

Preparation and characterization of crosslinked poly(vinylimidazolium) anion exchange membranes for artificial photosynthesis

Journal:	*Journal of Materials Chemistry A*
Manuscript ID	TA-ART-01-2019-000498.R1
Article Type:	Paper
Date Submitted by the Author:	11-Mar-2019
Complete List of Authors:	Carter, Blaine; Lawrence Berkeley National Laboratory, Joint Center for Artificial Photosynthesis Keller, Laura; RWTH Aachen University, Chemical Process Engineering Wessling, Matthias; RWTH Aachen University, Chemical Process Engineering; DWI-Leibniz Institute for Interactive Materials Miller, Daniel; Lawrence Berkeley National Laboratory, Joint Center for Artificial Photosynthesis

SCHOLARONE™
Manuscripts

Preparation and characterization of crosslinked poly(vinylimidazolium) anion exchange membranes for artificial photosynthesis

Blaine M. Carter[1], Laura Keller[2], Matthias Wessling[2,3], and Daniel J. Miller[1†]

†Corresponding Author, Tel: +1 (510) 495-2353 E-mail: danieljmiller@lbl.gov

[1]Joint Center for Artificial Photosynthesis, Lawrence Berkeley National Laboratory, Berkeley, CA 97420, United States

[2]RWTH Aachen University, Chemical Process Engineering, Forckenbeckstr. 51, 52074 Aachen, Germany

[3]DWI – Leibniz Institute for Interactive Materials, Forckenbeckstr. 50, 52074 Aachen, Germany

Abstract:

The interrelated nature of material properties in ion exchange membranes, such as ion exchange capacity and water uptake, frustrates the systematic study of how membrane chemistry and structure affect the transport of water, ions, and uncharged solutes in the membrane. Herein, we describe the preparation of a series of crosslinked poly(vinylimidazolium) anion exchange membranes by UV-photopolymerization of difunctional (*i.e.*, crosslinking) and monofunctional (*i.e.*, non-crosslinking) monomers, in which the ion exchange capacity and crosslink density may be independently controlled. Ion exchange membranes used in artificial photosynthesis (solar-driven CO_2 reduction) devices must permit the transport of electrolyte ions and minimize the crossover of CO_2 reduction products (*e.g.*, alcohols) between electrodes. The water content, methanol (CO_2 reduction product) permeability, and ionic conductivity of the membranes were evaluated. Ionic conductivity and methanol permeability were increased by reducing crosslink density or increasing solvent in the prepolymerization solvent mixture. For all prepared membranes, methanol permeability was directly correlated with water volume fraction in the

membrane. Minimizing the water volume fraction is critical to the design of membranes with low permeability to CO_2 reduction products.

Keywords:
Ion exchange membrane, permeability, methanol, ionic conductivity, artificial photosynthesis

1. Introduction

Ion exchange membranes are broadly used in diverse applications, including energy storage, water treatment, and energy generation.[1–3] These membranes are often comprised of polymers with charged moieties covalently attached to the polymer backbone. Ion exchange membranes are critical components of many electrochemical devices and have consequently been the subject of study for many years, yet a complete understanding of how membrane chemical and structural characteristics affect transport properties has not been realized.[2] Understandably, most experimental effort has concentrated on understanding water and ion transport,[1] and recently, fundamental studies of uncharged solute (*e.g.*, alcohol) transport in ion exchange membranes have been reported.[4]

To understand how membrane chemistry and structure affect water, ion, and neutral solute transport, model polymer systems whose properties can be systematically varied through careful synthesis are desirable. A significant challenge in designing ion exchange polymer systems is that several material properties may be interrelated.[2] For example, the ion exchange capacity (IEC, moles of ions/g dry polymer) affects both the ionic conductivity and the water uptake of the polymer.[2,3,5] The substantial water uptake associated with large IEC values can lead to excessive swelling and a loss of mechanical stability.[3,5] Covalent crosslinking is an effective

tool to limit swelling and has been employed in numerous anion exchange materials.[5–7] Permeability to ions (*i.e.*, ionic conductivity), water, and neutral solutes typically decreases with an increase in crosslink density, while excessive crosslinking can result in a brittle membrane.[5,8] A model system that provides independent control over the IEC and crosslink density would enable decoupling of many of the aforementioned properties, but can be synthetically challenging because multiple chemical functionalities (*e.g.*, crosslinkable and non-crosslinkable moieties, charged moieties), must be incorporated.

An emerging technology that utilizes ion exchange membranes is artificial photosynthesis, the photoelectrochemical reduction of CO_2 to carbon-neutral fuels and chemicals by which fluctuating solar energy can be converted into chemical energy available on demand.[9] While CO_2 reduction to CO by, for example, the Fischer-Tropsch process for the purpose of syngas production is well known,[10] CO is not readily useful as a fuel.[11] Instead, the target of much ongoing artificial photosynthesis research is the direct production of hydrocarbon fuels or chemical feedstocks.[12,13] The simplest artificial photosynthesis device configuration consists of two half-cells, each containing a planar electrode and aqueous electrolyte, that are separated by an ion exchange membrane.[14] Carbon dioxide is reduced to alcohol or other products[11] at the cathode, while water is oxidized to O_2 at the anode. The membrane in these devices serves two functions: (a) permit the transport of electrolyte charge carriers between electrodes so that current can flow, and (b) minimize the crossover of CO_2 reduction products from the cathode to the anode, where CO_2 reduction products could be re-oxidized to CO_2. Commonly the electrolyte is near-neutral pH, but an alkaline environment is reported to promote carbon-carbon coupling and, therefore, the formation of C_{2+} products.[15,16] Major electrolyte charge carriers include bicarbonate, carbonate, and hydroxide ions. Consequently, anion exchange membranes that

contain covalently bound cationic groups are favorable, since these membranes readily transport these negatively charged ions.[16]

Selemion AMV is a commercial anion exchange membrane that is commonly employed in (photo)electrochemical CO_2 reduction studies.[16,17,39] Selemion AMV is fabricated by the "paste method," where a blend of poly(vinyl chloride) and functionalized poly(styrene) are applied to a poly(vinyl chloride) nonwoven support.[18] The poly(styrene) is thought to be functionalized with quaternary ammonium and pyridine moieties, although some uncertainty remains in the literature.[19,20] While Selemion AMV sees wide use in electrochemical studies,[11,21–23] this proprietary composite membrane does not serve as a tunable system with which structure–property relationships may be established. However, model polymers with chemical features inspired by Selemion AMV, such as charged aromatic heterocycles covalently bound to hydrocarbon backbones, could serve as useful analogs that enable systematic study of membrane properties governing transport in artificial photosynthesis devices. Imidazolium-based styrenic polymers for CO_2 reduction applications have recently been commercialized and employed in gas diffusion electrode type devices,[24–26] but systematic membrane structure-property studies have not been reported.

Difunctional (*i.e.*, crosslinkable) vinylimidazolium monomers with alkyl spacers (Figure 1a) have been investigated for a range of applications.[27–30] With a halide (*e.g.*, Cl^-, Br^-) counterion, these monomers are soluble in water or methanol and the resulting solution can be cured into crosslinked networks using an appropriate initiator. Monofunctional analogs of these materials (Figure 1b) have also been synthesized.[29,31,32] Mixing difunctional and monofunctional monomers of the same spacer length *n* allows variation of the crosslink density without changing the IEC. Because both crosslink density and IEC affect the water uptake of the polymer, we

propose that this system permits decoupling of the crosslink density and the IEC and, therefore, independent control of water uptake by crosslink density without changing the IEC. Furthermore, adjusting the spacer length *n* permits variation of both the crosslink density and IEC. To our knowledge, no investigations have been reported on combinations of these difunctional and monofunctional monomers to afford networks with control of both crosslink density and IEC.

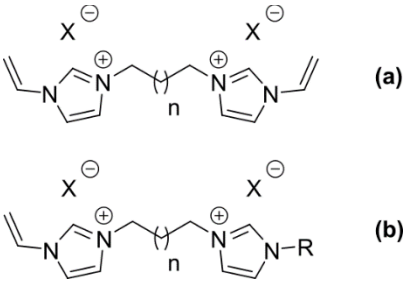

Figure 1. Structure of (a) difunctional vinylimidazolium monomers and (b) monofunctional vinylimidazolium monomers

Herein, we describe the systematic preparation and characterization of a series of anion exchange membranes based on the difunctional and monofunctional vinylimidazolium monomers shown in Figure 1. These membranes were prepared by UV-photopolymerization of aqueous or methanolic solutions of the vinylimidazolium monomers. By varying the monomer spacer length, crosslinker (*i.e.*, difunctional monomer) content, and prepolymerization solvent content, membranes with a variety of crosslinked network structures were prepared at fixed IECs. The membranes were characterized by measuring the equilibrium water content, methanol permeability, and ionic conductivity. Because methanol is among the smallest reported CO_2 reduction products, it is a challenging solute of which to limit transport across a membrane. Furthermore, straightforward techniques for measurement of methanol permeation have been established using *in situ* FTIR spectroscopy.[33,34] Trends in the prepared membrane properties are

discussed, as well as the relationship between water volume fraction in the membrane and permeability to ions and solutes.

2. Experimental

2.1 Materials

N-Vinylimidazole (98%), *N*-methylimidazole (99%), 1,12-dibromododecane (98%), eicosanedioic acid (98%), carbon tetrabromide (99%), 2-hydroxy-4'-(2-hydroxyethoxy)-2-methylpropiophenone (Irgacure 2959, 98%), were purchased from TCI America and used as received. Borane tetrahydrofuran complex (1 M) and triphenylphosphine (99%) were purchased from Alfa Aesar and used as received. Methanol (reagent grade, ≥ 99.5% purity) was purchased from Sigma-Aldrich and used as received. Ultrapure water was supplied by an EMD Millipore Milli-Q Integral 3 water purification system (18.2 MΩ•cm at 25 °C, 1.2 ppb TOC). All other reagents and solvents were ACS Reagent Grade or higher quality.

2.2 Synthesis of vinylimidazolium monomers

Monomers **1**, **2**, **1a**, and **2a** were synthesized according to Scheme 1. Details of the synthesis are described in the subsequent sections. NMR spectra (^{1}H and ^{13}C) for all compounds are provided in the Supporting Information.

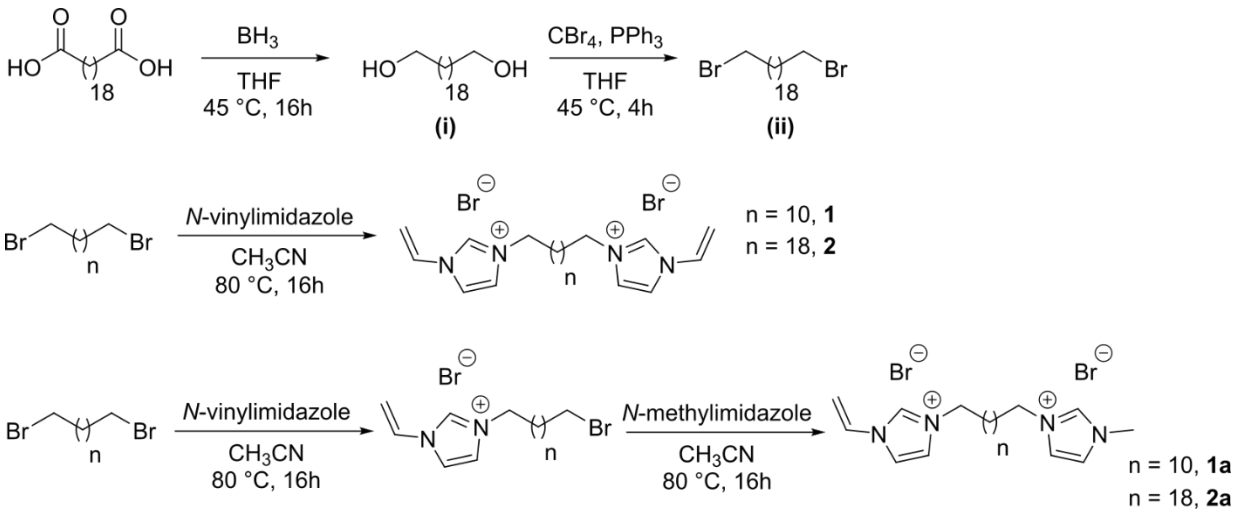

Scheme 1. Synthesis of monomers **1**, **2**, **1a**, and **2a**

*2.2.1 Synthesis of 1,20-eicosanediol **(i)***

Anhydrous THF (500 mL) and borane-THF complex (100 mL, 100 mmol) were added to a 1000 mL round-bottom flask equipped with a stir bar and reflux condenser under flowing nitrogen. Eicosanedioc acid (11.41 g, 33.3 mmol) powder was added slowly to the reaction mixture to minimize bubbling and the resultant slurry was heated to 45 °C for 16 hours. After cooling to room temperature, the reaction was quenched with H_2O (15 mL) dropwise. Diethyl ether (300 mL) was added, followed by dropwise addition of 4 M NaOH (20 mL). The organic layer was washed with H_2O (3 × 50 mL), then with brine (3 × 50 mL), and then dried over anhydrous $MgSO_4$. The $MgSO_4$ was rinsed with additional warm (ca. 30 °C) THF (500 mL). The resulting organic solution was reduced under rotary vacuum to afford a white solid. The solids were stirred in a H_2O/MeOH solution (200 mL, 60/40 (v/v)) for 20 minutes, filtered, and dried in a vacuum oven (< 1 Torr, 40 °C) to afford 1,20-eicsoanediol as a white powder (10.25 g, 32.6 mmol, 98 % yield). NMR spectra for this compound matched published data.[35]

*2.2.2 Synthesis of 1,20-dibromoeicosane (**ii**)*

The procedure to synthesize 1,20-dibromoeicosane was adapted from an analogous reaction described in the literature.[36] Anhydrous THF (100 mL) was added to a 250 mL round-bottom flask equipped with a stir bar and reflux condenser under flowing nitrogen. After heating the solvent to 45 °C, carbon tetrabromide (12.65 g, 38.1 mmol) and 1,20-eicosanediol (3.00 g, 9.5 mmol) were added. Triphenylphosphine (14.15 g, 53.9 mmol) was added slowly over the course of 30 minutes. After stirring for 4 hours at 45 °C, the resultant mixture was cooled to room temperature and the solids were removed *via* filtration. Residual THF was removed under rotary vacuum to afford an orange solid. The solids were stirred in a H_2O/EtOH solution (200 mL, 40/60 (v/v)) overnight. The solids were collected by filtration and rinsed with H_2O/EtOH solution (200 mL, 40/60 (v/v)). After drying the solids (3.43 g) in a vacuum oven (< 1 Torr, 40 °C), ^{1}H NMR typically indicated that a small amount of unreacted alcohol remained. A similar procedure was used to convert the remaining alcohols. Anhydrous THF (50 mL) was added to a 100 mL round-bottom flask equipped with a stir bar under flowing nitrogen. The product mixture (3.43 g) and carbon tetrabromide (6.32 g, 19.1 mmol) were added, followed by slow addition of triphenyphosphine (7.03 g, 26.8 mmol). After 1 hour, solids were filtered and THF was removed under rotary vacuum. The solids were stirred in a H_2O/EtOH solution (200 mL, 40/60 (v/v)) three times, filtered, and dried in a vacuum oven (< 1 Torr, 40 °C) to afford the product as a white powder (3.16 g, 7.2 mmol, 76 % yield).

*2.2.3 Synthesis of monomer **1***

1,12-Dibromododecane (4.98 g, 15.2 mmol), *N*-vinylimidazole (3.03 g, 32.2 mmol), and acetonitrile (7 mL) were combined in a 50 mL round-bottom flask equipped with a stir bar and

reflux condenser. The reaction solution was heated to 70 °C for 16 hours. The solidified reaction mixture was cooled to room temperature and mixed with acetone (100 mL). Filtering the solution afforded the product as a white solid (6.75 g, 13.1 mmol, 86 % yield). NMR spectra for this compound matched published data.[37]

*2.2.4 Synthesis of monomer **2***

1,20-Dibromoeicosane (2.49 g, 5.7 mmol) was mixed with acetonitrile (11 mL) and toluene (3.5 mL) in a 25 mL round-bottom flask equipped with a stir bar and reflux condenser. The mixture was heated to 55 °C and *N*-vinylimidazole (2.32 g, 24.7 mmol) was added. The homogenous solution was heated to 80 °C for 16 hours. Upon cooling to room temperature, a white precipitate formed and the slurry was poured into diethyl ether (300 mL). The solids were filtered, rinsed with diethyl ether (100 mL), and dried under vacuum (< 0.1 Torr) to afford the product as a white powder (3.37 g, 5.4 mmol, 94 % yield).

*2.2.5 Synthesis of monomer **1a***

1,12-Dibromododecane (30.05 g, 91.6 mmol) was mixed with acetonitrile (30 mL) in a 100 mL round-bottom flask equipped with a stir bar and reflux condenser. The solution was heated to 55 °C to produce a homogenous solution. *N*-Vinylimidazole (1.54 g, 16.4 mmol) was added dropwise and then the mixture was heated to 80 °C for 16 hours. The reaction mixture was cooled to room temperature and hexanes (15 mL) was added. The product was extracted into methanol (50 mL) and washed with hexanes (5 × 100 mL). Methanol was removed by rotary vacuum to afford a viscous brown liquid. The product was washed with diethyl ether (2 × 150 mL) and hexanes (2 × 100 mL). After sitting in hexanes for approximately 30 minutes, the

product solidified. The solids were washed with fresh hexanes (100 mL), filtered, and dried under vaccum (< 0.1 Torr) to afford the intermediate product as a white powder (5.96 g).

The intermediate product (5.96 g) was mixed with acetonitrile (16 mL) and heated to 50 °C. *N*-Methylimidazole (1.5 g, 18.3 mmol) was added and the reaction mixture heated to 80 °C for 16 hours. After cooling to room temperature, acetonitrile was removed by rotary vacuum, yielding a light brown viscous liquid. The product was washed with ethyl acetate (2 × 100 mL) and diethyl ether (2 × 100 mL). After sitting in diethyl ether for approximately 30 minutes, the product solidified. After decanting, the solids were washed with fresh diethyl ether (100 mL). The product was hygroscopic, so the diethyl ether slurry was transferred to a Schlenk flask. Excess diethyl ether was decanted and the solids were dried under vacuum (< 0.1 Torr) to afford the product as a white powder (6.75 g). This procedure results in a mixture of monomers **1** and **1a**. The ratio of these two compounds was calculated from ^{1}H NMR as described in the Supporting Information. With this procedure, a typical concentration of monomer **1** was 6 mol %.

*2.2.6 Synthesis of monomer **2a***

1,20-Dibromoeicosane (3.25 g, 7.4 mmol) was mixed with acetonitrile (6 mL) and toluene (4 mL) in a 25 mL round-bottom flask equipped with a stir bar and reflux condenser. The mixture was heated to 55 °C and *N*-vinylimidazole (0.41 g, 4.5 mmol) was added dropwise. The homogenous solution was heated to 75 °C for 16 hours. Upon cooling to room temperature, methanol (10 mL) and hexanes (10 mL) were added. The methanol layer was washed with hexanes (5 × 50 mL), and then the methanol was removed by rotary vacuum. The resulting white

solid was stirred in hexanes (100 mL), filtered, rinsed with hexanes (2 × 100 mL), and dried under vacuum (< 0.1 Torr) to afford the intermediate product as a white powder (1.52 g).

The intermediate product (1.52 g) was mixed with acetonitrile (4 mL) and heated to 70 °C. *N*-Methylimidazole (0.32 g, 3.8 mmol) was added and the reaction mixture heated to 80 °C for 16 h. On cooling to room temperature, a white precipitate formed and diethyl ether was added (200 mL). The solids were filtered, rinsed with diethyl ether (100 mL), and dried under vacuum (< 0.1 Torr) to afford the product as a white powder (1.62 g). This procedure results in a mixture of monomers **2** and **2a**. The ratio of these two compounds was calculated from ^{1}H NMR as described in the Supporting Information. With this procedure, a typical concentration of monomer **2** was 25 mol %.

2.3 Membrane preparation

Appropriate amounts of monomer, solvent, and photoinitiator (0.1 wt. % relative to monomer) were added to a small vial. The contents were gently heated to dissolve the monomer, thoroughly mixed, and the resultant solution was filtered through a 0.45 μm PTFE filter. Two quartz plates were treated with Rain-X® according to manufacturer's instructions and wiped clean with a Kimwipe to remove excess Rain-X®. The plates were then pre-heated on a temperature-controlled hot plate to the desired temperature. Temperatures for all mixtures are specified in the Supporting Information. Steel spacers (50 or 100 μm) in between the quartz plates were used to control the film thickness.

The prepolymerization mixture was heated to 80 °C and transferred by pipette onto a pre-heated (80 °C) quartz plate and quickly covered with a second pre-heated (80 °C) quartz plate. The sample was irradiated with a 365 nm UV lamp (3 mW cm^{-2} at the sample surface) for 20

minutes. The films were removed from the quartz plates and soaked in ultrapure water. Films were equilibrated in fresh ultrapure water for 24 hours before characterization.

A high degree of conversion (> 90 %) for all samples was confirmed using attenuated total reflectance Fourier transform infrared (ATR FTIR) spectroscopy. Films used for ATR FTIR analysis were not soaked in water after curing, but immediately transferred to an empty glass jar and dried in a vacuum oven (< 1 Torr, 40 °C) for 24 hours. The dried film spectra were compared with the neat monomer mixture. Disappearance of the peaks at 1648 cm^{-1} and 945 cm^{-1}, corresponding to the vinyl moiety participating in crosslinking, demonstrated high conversion. ATR FTIR spectra are provided in the Supporting Information.

2.4 Conversion of Selemion AMV membrane to bromide form

Selemion AMV membrane (AGC Engineering Co., Ltd., Chiba, Japan) is supplied in the chloride form (*i.e.*, the counter ions to the cationic moieties in the membrane are chloride ions).[19] The as-delivered membrane was converted to the bromide form by soaking in 1 M NaBr solution for 48 h with refreshment of the soaking solution every 12 hours. The Selemion AMV membranes were then soaked in ultrapure water for 24 hours, refreshing the ultrapure water after 12 hours of soaking.

2.5 Water content

The water content of equilibrated membranes was measured by liquid sorption.[38,39] Hydrated samples were quickly blotted between two pieces of Kimwipe and weighed, W_h. The films were then dried under vacuum (< 1 Torr, 40 °C) to constant weight (minimum 24 h) and

weighed again to determine the mass of the dry film, W_d. The percent water content, ω_W, was calculated as follows:

$$\omega_W = \frac{W_h - W_d}{W_h} \times 100\%$$

2.6 Polymer density

The density of the dry polymer, ρ_d, was measured using a gas pycnometer (AccuPyc II 1340, Micromeritics, Norcross, GA). The sample holder was dried at 120 °C and ambient pressure and then quickly weighed. All samples were dried under vacuum (< 1 Torr, 40 °C) overnight. Subsequently, they were cut into small squares approximately 5 mm x 5 mm in size, added to the sample holder, and then dried under vacuum (< 1 Torr, 40 °C) for a minimum of 24 h. Upon removal from the oven, the sample was weighed and quickly transferred to the pycnometer to minimize water uptake from the atmosphere. The density measurement was carried out using ten purge cycles and ten measuring cycles with helium. The pressure change for each measurement step was ≤ 0.005 psi/min before a value was taken and the next measurement step started. For each monomer, the polymer density was determined for three membranes samples prepared at three different prepolymerization solvent contents and the average was used for subsequent calculations.

2.7 Calculation of water volume fraction

Assuming volume additivity, which has been shown to be reasonable for a number of charged polymers,[40,41] the water volume fraction in the fully hydrated film, ϕ_w, was calculated using the measured polymer density, ρ_P, and both the dry and hydrated weight of the films:

$$\phi_w = \frac{(W_h - W_d)/\rho_W}{(W_h - W_d)/\rho_W + W_d/\rho_p}$$

The density of water, ρ_W, was taken as 1.0 g/mL.

2.8 Methanol permeability measurements

Methanol permeability was measured using a standard diffusion cell (Adams and Chittenden Scientific Glassware, Berkeley, CA) equipped with an ATR FTIR probe (Mettler-Toledo ReactIR™ 15 with shallow tip 9.5 mm DSub AgX DiComp probe) in the receiver cell. A full description of this experimental apparatus and method is reported elsewhere.[33,34] All experiments were performed at 25 °C with an initial donor cell concentration of 1 M methanol. Spectra were collected until the receiver cell concentration reached a minimum concentration of 75 mM. Permeability measurements were conducted on three individually prepared membranes and the reported error is the standard deviation of these replicates.

2.9 Ionic conductivity measurements

In-plane conductivity was measured using a four point conductivity cell (BekkTech BT-110) interfaced with a Biologic VSP-300 potentiostat. A rectangular section of membrane (length: > 2.5 cm, width: 0.8 - 1.3 cm) was cut and mounted in the cell, and then the cell was immersed in ultrapure water (300 mL). Linear sweep voltammetry (-0.1 V to +0.1 V, 10 mV/s) was performed. The resistance, R (Ω), is the slope of the voltage vs. current curve. Ionic conductivity was calculated from $\sigma = L/RWT$, where σ is the ionic conductivity (S/cm), L is the distance between the sensing electrodes (0.45 cm), and W and T are the width and thickness of the membrane, respectively. Conductivity measurements were made on three individually prepared membranes and the reported error is the standard deviation of these replicates. Prior

publications have reported similar in-plane and through-plane ionic conductivity values for solution-cast isotropic polymer electrolyte membranes;[42] future contributions will report the performance of the membranes described here in electrochemical cells.

3. Results and Discussion

3.1 Equilibrium water content of membranes

The diffusion of small molecules in hydrated polymers is described by free volume theory, by which solutes diffuse by executing jumps among interstitial voids that open as a result of polymer segmental motion.[43,44] In water-swollen polymers, Yasuda et al.[44] proposed and showed to a first approximation that the water in a hydrated polymer fills the available free volume. Measurement of the equilibrium water content, therefore, provides insight into the free volume in the membrane and forms a basis for understanding differences in transport properties among membranes.

A series of free-standing, unsupported membranes were prepared with monomers **1** and **2** by varying solvent content in the prepolymerization mixture. At mild temperatures, monomer **1** is soluble in both methanol and water, while monomer **2** is soluble in methanol, but only slightly soluble in water. As a result, no membranes of monomer **2** were prepared in water. After preparation, membranes were equilibrated in water.

Figure 2(a) shows how the equilibrium water content varied in these membranes with prepolymerization solvent content (reported here in terms of solvent weight percent for congruity with prior publications[45]). In general, water content in the membrane increased with increasing prepolymerization solvent content. For membranes prepared in water, it is useful to compare the water content with the parity line (the dotted line in Figure 2(a)), which indicates the case where

the equilibrium water content in the prepared membrane was identical to the prepolymerization water content. Only one of the membranes of monomer **1** prepared in water at 12.5 wt. % fell on the parity line. To ensure the solubility of monomer **1** at this low water content, the solution and the quartz plates used for the membrane preparation were heated to 80°C (see Table S1). The preparation of membranes with lower water contents necessitated higher temperatures (near the solvent boiling point) and did not yield reproducible results.

All other membranes of monomer **1** prepared in water fell below the parity line, which means that the membrane contained less water than the initial prepolymerization mixture. The decrease in water content could be due to polymerization-induced phase separation.[46,47] As the polymer network formed and the crosslink density increased, swelling of the network was restricted and excess solvent forced out. Even though excess solvent is forced out during polymerization, only two films were cloudy after polymerization, suggesting a heterogeneous structure. Membranes prepared with monomer **1** using 50 wt. % water and monomer **2** using 50 wt % methanol transitioned from transparent to translucent as the polymerization progressed. All other prepared membranes were optically transparent and uniform after polymerization.

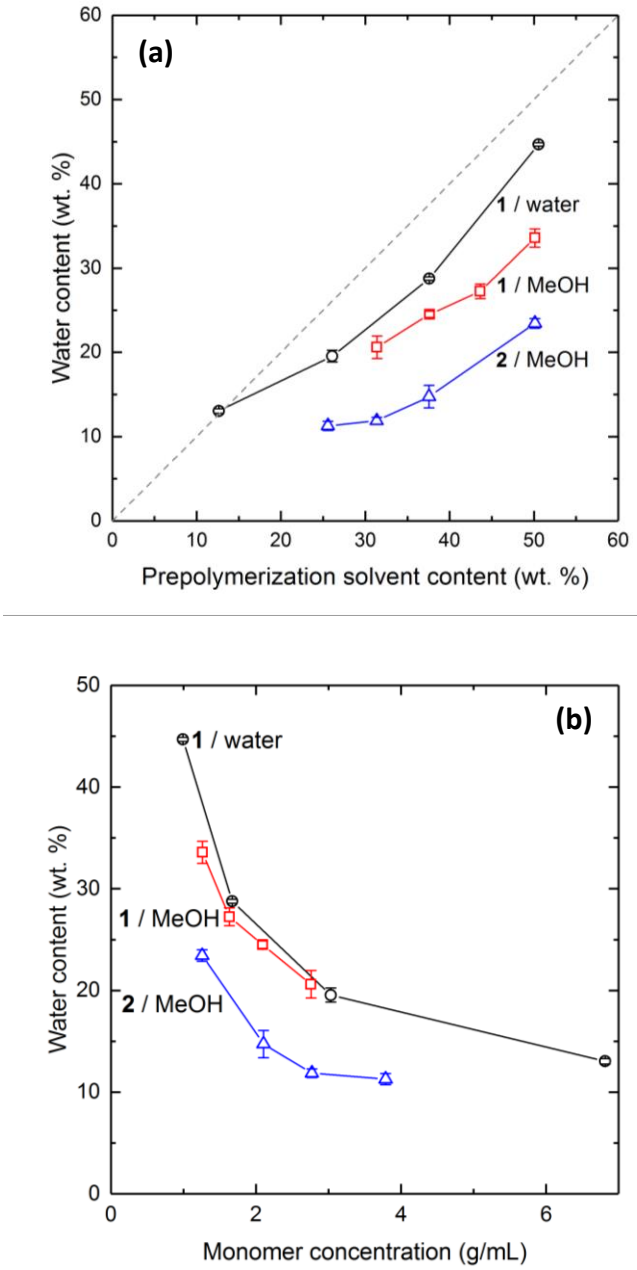

Figure 2. (a) Equilibrium water content of membranes prepared with monomer **1** and **2** as a function of prepolymerization solution solvent content. The dashed line is the parity line, where the equilibrium water content is equal to the prepolymerization solvent content. (b) Equilibrium water content of membranes prepared with monomers **1** and **2** as a function of prepolymerization solution monomer concentration.

For membranes prepared in methanol, the solvent was exchanged for water after polymerization. Since the densities of methanol and water differ, it is useful to compare the equilibrium water contents of the membranes as a function of prepolymerization monomer concentration (Figure 2(b)). The equilibrium water content was similar for membranes prepared with monomer **1** in water and in methanol for a given monomer concentration (in g monomer per mL prepolymerization solution). This result suggests that the *volume* fraction of solvent in the prepolymerization solution (rather than the *weight* fraction) plays an important role in determining the equilibrium water content. Correlation of transport properties with sorbed water volume fraction in crosslinked films will be discussed later.

For similar monomer concentrations, membranes prepared with monomer **2** had lower equilibrium water content than membranes prepared with monomer **1**. One simple explanation for this result is that the longer hydrocarbon spacer in monomer **2** contributes to greater hydrophobicity, leading to lower water uptake. However, the crosslink density and IEC in these systems are also expected to affect the equilibrium water uptake.[5] In difunctional monomers **1** and **2**, an ionic imidazole moiety is associated with each reactive vinyl moiety. At a fixed pre-polymerizaton solvent content and degree of polymerization (essentially 100% in all of the polymers described here), polymers synthesized from monomer **1** were expected to have a higher crosslink density than those synthesized from monomer **2**, since the spacer in monomer **1** was shorter than that in monomer **2.** However, polymers prepared from monomer **1** were also expected to have a higher IEC than polymers prepared from monomer **2** due to the lower molecular weight of monomer **1**. Based on the molecular weight and number of charged groups, the IEC of membranes prepared with monomer **1** was 3.87 mmol/g, whereas the IEC was 3.18

mmol/g for membranes prepared with monomer **2**. An increase in IEC is expected to increase swelling,[5] but in this system, an increase in IEC was accompanied by an increase in crosslink density, which can limit swelling.[5] Despite these competing effects, the longer hydrocarbon spacer in monomer **2** resulted in lower equilibrium water content in polymers prepared from monomer **2** than in polymers prepared form monomer **1**.

The effect of crosslinker content on membrane water content was examined by mixing difunctional monomers (**1** and **2**) with monofunctional monomers (**1a** and **2b)**. Difunctional monomer content was varied from 25 mol % to 100 mol % and prepolymerization solvent content was the same for each pair (**1**/**1a** or **2**/**2a**) of monomers. For monomers **1** and **1a**, membranes were prepared with a prepolymerization mixture containing 25 wt. % water. For monomers **2** and **2a**, membranes were prepared with a prepolymerization mixture containing 37.5 wt. % methanol. These prepolymerization solvent concentrations were chosen because the methanol permeabilities of membranes prepared using only difunctional mononomers at these concentrations were comparable to commercial Selemion AMV (see section 3.2).

Figure 3 shows that the equilibrium water content of membranes prepared from both monomer pairs decreased as the crosslinker (*i.e.*, difunctional monomer) content increased. This result suggests that the amount of water sorbed by the polymer network was limited by the degree of crosslinking. For monomers **1** and **1a**, reducing the crosslinker content to 25 mol % resulted in membranes that sorbed more water than was present in the prepolymerization mixture (*i.e.*, this membrane would be above the parity line in Figure 2a). While membrane pliability qualitatively improved somewhat by decreasing crosslinker content, all of the membranes were easy to handle.

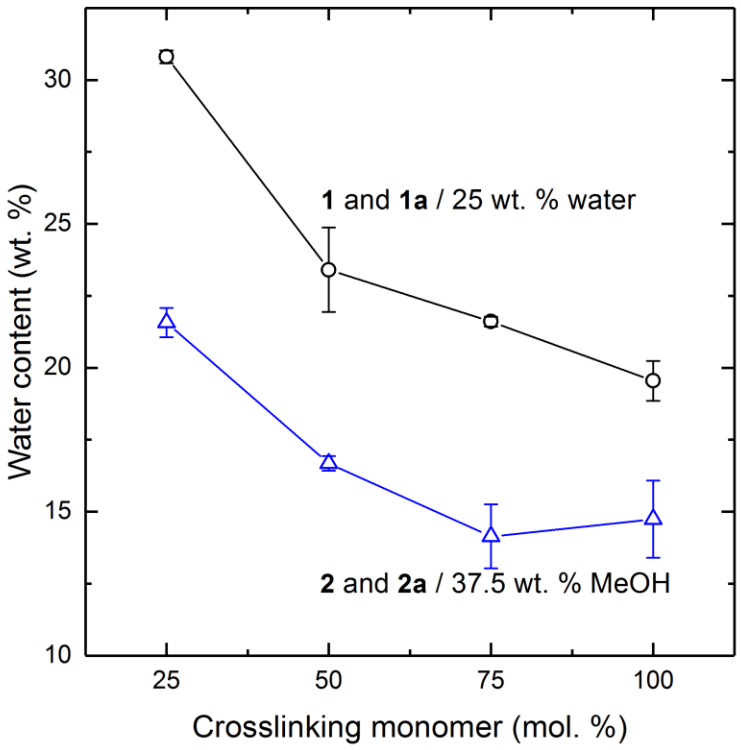

Figure 3. Equilibrium water content of membranes prepared with varying crosslinker content. Membranes of monomer **1** and **1a** were prepared with a prepolymerization solvent content of 25 wt. % water. Membranes of monomer **2** and **2a** were prepared with a prepolymerization solvent content of 37.5 wt. % methanol.

3.2 Methanol permeability of membranes

Methanol is an attractive target product for CO_2 reduction, as it could serve as a substitute for petroleum-derived liquid fuels, or as a feedstock for chemical synthesis.[48,49] While longer C_{2+} hydrocarbons are desirable end products of CO_2 reduction, methanol has been reported as a product of CO_2 reduction on copper and other catalysts.[11,49] Methanol is a useful "worst case" permeant for the present study because it is the smallest of the alcohols, making it an especially

challenging solute of which to limit the transport in a polymeric membrane. Furthermore, there is considerable interest in controlling methanol permeation through polymer electrolyte membranes in direct methanol fuel cells.[50–52] Straightforward permeation measurements of methanol through hydrated membranes have previously been established using *in situ* FTIR spectroscopy.[33,34]

Methanol permeability measurements were performed on free-standing, unsupported membranes prepared from monomers **1** and **2**. As shown in Figure 4(a), increasing the prepolymerization solvent content significantly increased the methanol permeability. For a given prepolymerization solvent content, membranes prepared with monomer **2** exhibited much lower methanol permeabilities than membranes with monomer **1**. Figure 4(b) shows the methanol permeability as a function of monomer concentration. Re-casting the data in terms of monomer concentration on the basis of prepolymerization solvent volume causes the methanol permeability values for membranes prepared using monomer **1** in both water and methanol solvents to converge. This result reinforces the assertion made in section 3.1 that prepolymerization solvent volume influences the total water uptake in these membranes and ultimately governs solute transport (cf., Figures 2(a) and 2(b)).

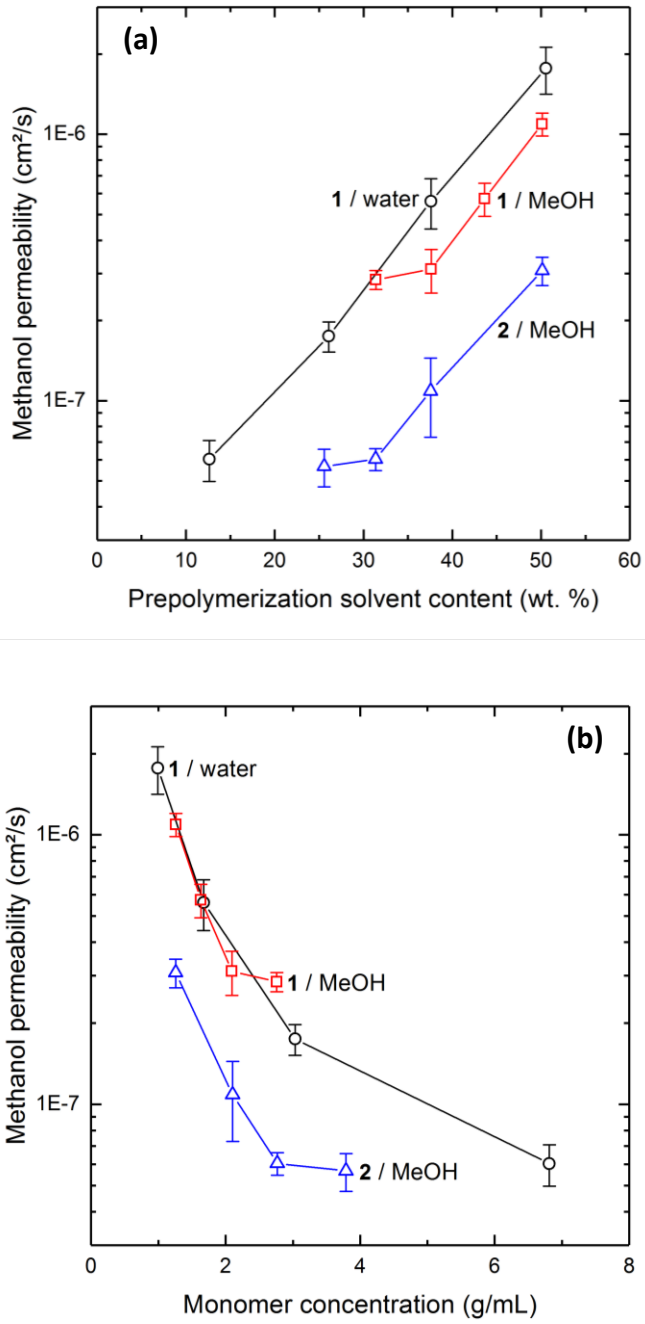

Figure 4. (a) Methanol permeability of membranes made with monomers **1** and **2** as a function of prepolymerization solution solvent content. (b) Methanol permeability of membranes made with monomers **1** and **2** as a function of prepolymerization solution monomer concentration.

The effect of crosslinker content on methanol permeability was explored by varying the difunctional monomer content at a fixed prepolymerization solvent content. As shown in Figure 5, increasing the crosslinker content resulted in a decrease in methanol permeability for both monomer systems. The relative decrease in methanol permeability was similar for both monomer systems.

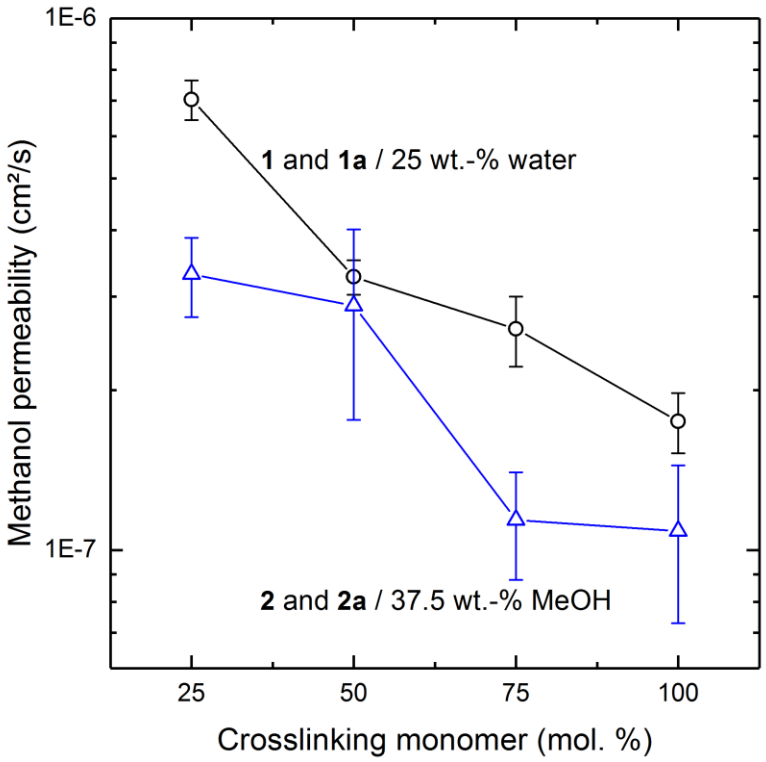

Figure 5. Methanol permeability of membranes with varying crosslinker content. Membranes of monomer **1** and **1a** were prepared with a prepolymerization solvent content of 25 wt. % water. Membranes of monomer **2** and **2a** were prepared with a prepolymerization solvent content of 37.5 wt. % methanol.

For all of the prepared membranes, trends in methanol permeability correlated with equilibrium water content measurements. Yasuda et al.[44] proposed that hydration of a swollen polymer is proportional to its free volume, and showed to a first approximation that polymer hydration is correlated with diffusive solute transport. Specifically, the diffusion coefficient of a solute in a swollen polymer $\overline{D_i}$ can be expressed as a function of water volume fraction:

$$\overline{D_i} = D_{0,i}\exp\left[-A\left(\frac{1}{\phi_w}-1\right)\right]$$

where $D_{0,i}$ is the solute diffusivity in pure water, ϕ_w is the volume fraction of water in the polymer, and A is an empirical constant.[38] This model is most applicable to small solutes (salt ions and small organic molecules) in dilute and semi-dilute (*i.e.*, highly hydrated) polymer systems.[43]

The solution-diffusion model teaches that the permeability of a hydrated polymer to a solute is the product of the solute diffusivity and solubility in the polymer.[53] Yasuda et al. showed that variations in solute diffusivity that arise with changes in polymer water volume fraction often strongly affect solute permeation.[38,44] As a result, permeability is often highly dependent on polymer water volume fraction.

In order to understand the methanol permeability measurements in the context of free volume theory, it was necessary to convert equilibrium water content (Section 3.1) to water volume fraction. Assuming volume additivity, which has been shown to be reasonable for several charged polymers,[40,41] water volume fraction is easily calculated using water weight fraction and polymer density. The density of polymers prepared with monomer **1** was 1.42 g/mL, whereas it was 1.35 g/mL for polymers prepared with monomer **2**. The measured density did not vary significantly with prepolymerization solvent content.

As shown in Figure 6, the methanol permeability of all prepared membranes varied exponentially as a function of inverse water volume fraction ($1/\phi_w$). Interestingly, this correlation holds for all of the prepared membranes, regardless of the monomer spacer length or crosslinker content. This result suggests that overall polymer free volume (as indicated by the water volume fraction) is the primary governor of methanol permeability, and that the permeability is otherwise insensitive to the details of network structure or polymer chemistry. Assuming this relationship extends outside the studied range of water volume fractions, further decreases in methanol permeability could be achieved with additional small decreases in water volume fraction. The lowest water volume fraction of the prepared membranes was $\phi_w = 0.15$. Decreasing the water volume fraction to approximately $\phi_w = 0.10$ could decrease the methanol permeability by another order of magnitude.

For a benchmarking comparison, the dotted line in Figure 6 is the measured methanol permeability of commercial Selemion AMV in the bromide form. The water volume fraction of Selemion AMV has not been measured and the methanol permeability is therefore represented as a horizontal line rather than a single point in Figure 6. Several of the prepared membranes had lower methanol permeabilities than to Selemion AMV. In principal, these membranes could be more effective at limiting the crossover of CO_2 reduction products in a device.

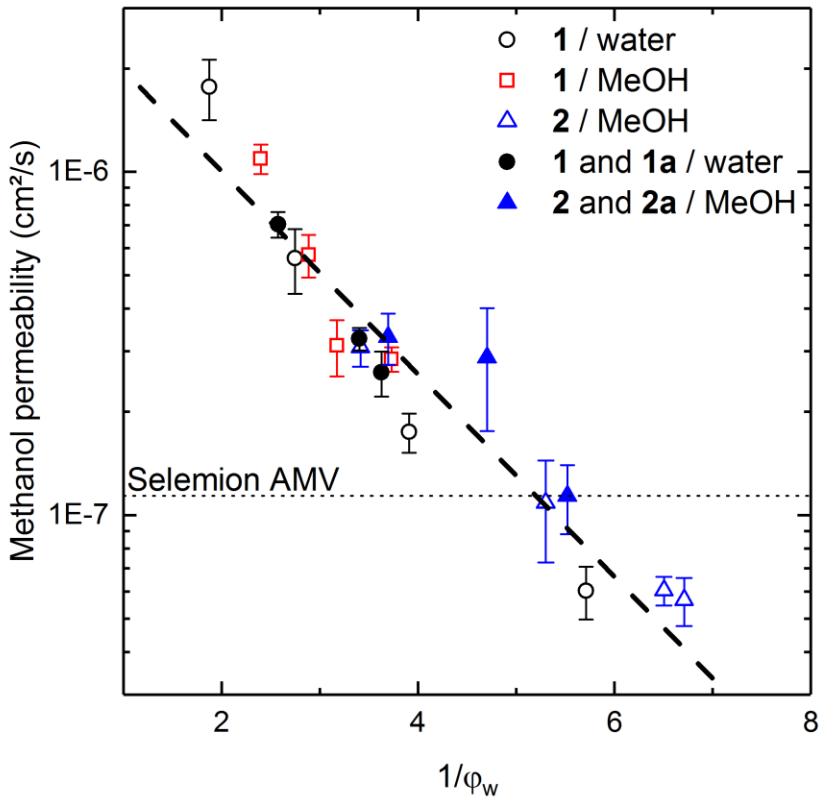

Figure 6. Methanol permeability of prepared membranes as a function of inverse water volume fraction. The thick dashed line is a line of best fit for all of the prepared membranes, which demonstrates a correlation of methanol permeability with inverse water volume fraction. For comparison, the thin dotted line is the methanol permeability of commercial Selemion AMV anion exchange membrane, exchanged to the bromide form.

3.3 Ionic conductivity of membranes

Ionic conductivity measurements were made on membranes prepared under the same conditions as described in Sections 3.1 and 3.2. As shown in Figure 7(a), ionic conductivity generally increased with increasing prepolymerization solvent content and, therefore, water

content. However, membranes prepared with monomer **1** at 50 wt. % water and monomer **2** at 50 wt. % methanol showed a plateau in ionic conductivity between 40 and 50 wt. % prepolymerization solvent content. Interestingly, the membrane prepared with monomer **1** using 50 wt % water and the membrane prepared with monomer **2** using 50 wt % methanol were both cloudy after polymerization. The heterogeneous structure of these two films may explain the deviation of these two membranes from the conductivity trend exhibited by the other membranes. Other reports on anion exchange membranes have shown ionic conductivity commonly increases with water content, but the structure and nature of the polymer and charged group are also critical factors.[5,41,54,55]

Ionic conductivities of membranes prepared with monomer **1** were moderately higher than those of membranes prepared with monomer **2**. This result is not surprising, since membranes prepared from monomer **2** had a lower IEC (3.18 mmol/g for monomer **2** vs. 3.87 mmol/g for monomer **1**) and water content than membranes prepared from monomer **1**.

Figure 7(b) shows the ionic conductivity as a function of monomer concentration. Similar to the results shown in Figures 2(b) and 4(b), ionic conductivities of membranes prepared using monomer **1** in water and methanol converged when plotted as a function of monomer concentration, again highlighting the importance of prepolymerization solvent volume in controlling membrane transport properties.

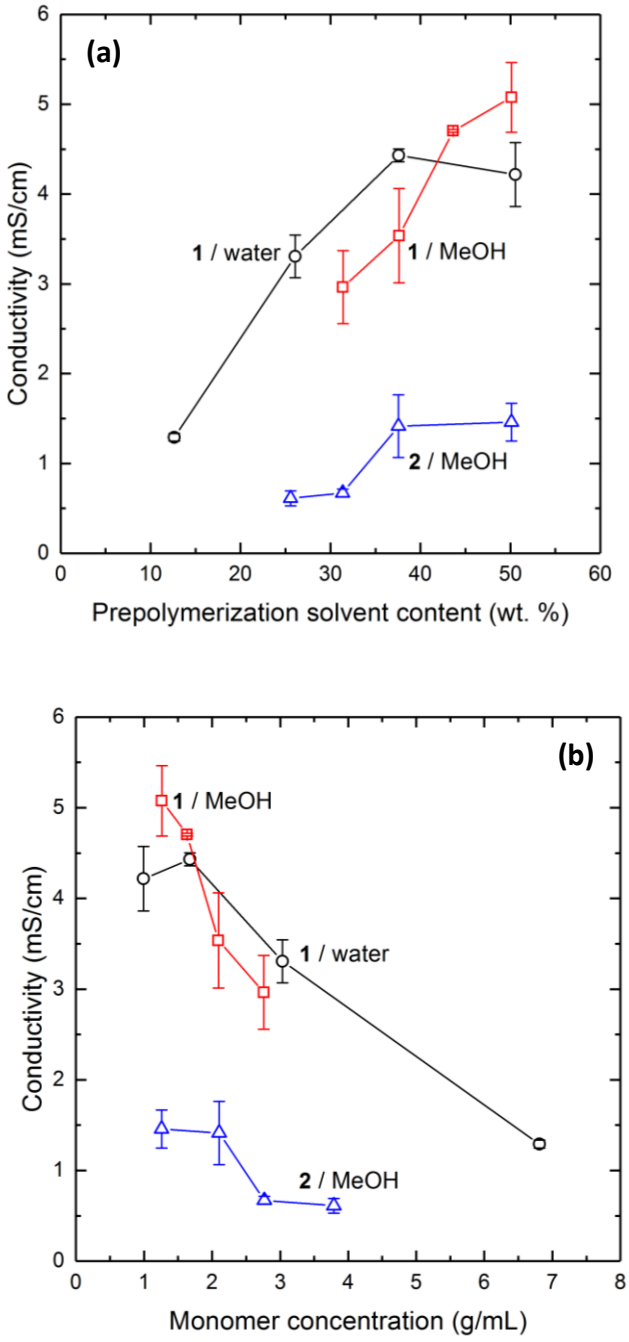

Figure 7. (a) Ionic conductivity of membranes prepared with monomers **1** and **2** as a function of prepolymerization solution solvent content. (b) Ionic conductivity of membranes prepared with monomers **1** and **2** as a function of prepolymerization solution monomer concentration.

The effect of crosslinker content on ionic conductivity is shown in Figure 8. As the amount of difunctional crosslinking monomer was increased, the ionic conductivity decreased. Relative decreases in conductivity were similar for both monomer systems. This decrease in conductivity with increasing crosslinker content is likely attributable to the decrease in water content observed with increasing crosslinker content (Figure 3).

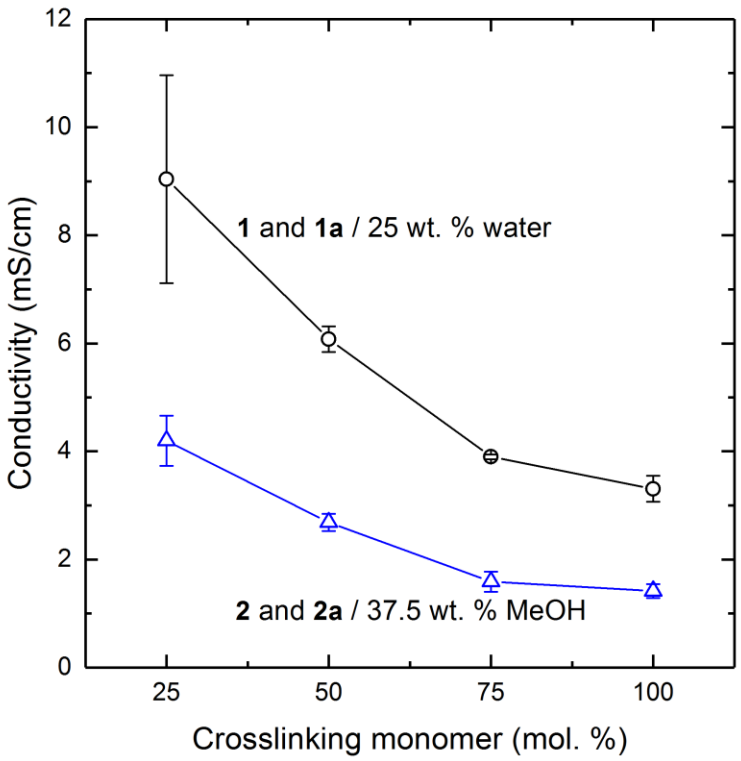

Figure 8. Ionic conductivity of membranes as a function of crosslinker content. Membranes of monomer **1** and **1a** were prepared with a prepolymerization solvent content of 25 wt. % water. Membranes of monomer **2** and **2a** were prepared with a prepolymerization solvent content of 37.5 wt. % methanol.

Like permeability measurements discussed in the previous section, it is useful to examine conductivity as a function of inverse water volume fraction for different membranes. As shown in Figure 9, the maximum ionic conductivities over a range of water volume fractions exhibited an exponential correlation with inverse water fractions (shown as a dashed line). Robeson et al. described the empirical relationship between maximum ionic conductivity and water sorption in proton exchange membranes as an "upper bound", where a trade-off relationship exists between conductivity and water sorption.[56] Similarly, Geise et al. investigated anion exchange membranes based on functionalized poly(phenylsulfone) and poly(2,6-dimethyl-1,4-phenylene oxide) and observed an analogous dependence of conductivity on inverse water volume fraction.[41] Membranes prepared in this study exhibit conductivity trends consistent with these descriptions.

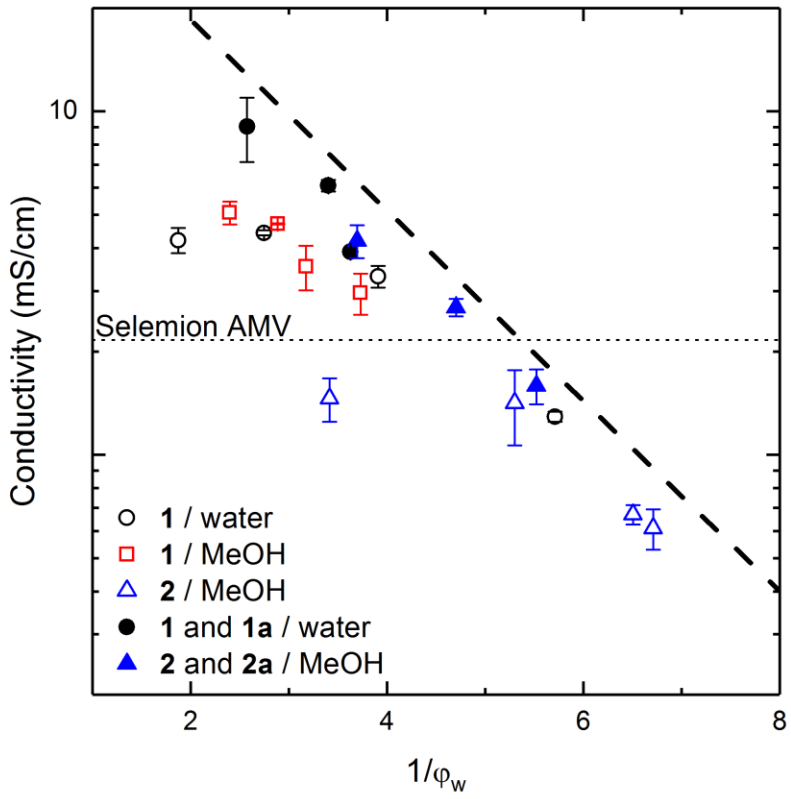

Figure 9. Ionic conductivity of all prepared membranes as a function of inverse water volume fraction. The thick dashed line is a qualitative "upper bound" relating the maximum exhibited ionic conductivities of this family of membranes to inverse water volume fraction. For comparison, the thin dotted line is the ionic conductivity of commercial Selemion AMV anion exchange membrane, exchanged to the bromide form.

For a benchmarking comparison, the dotted line in Figure 9 is the conductivity of commercial Selemion AMV (exchanged to the bromide form). Although the water volume fraction of Selemion AMV has not been measured, the IEC has been measured to be 1.85 mmol/g.[19] This is significantly lower than the IEC of all membranes prepared in this study (3.18

mmol/g for monomer **2**/**2a**, 3.87 mmol/g for monomer **1**/**1a**). Many of the prepared membranes had higher ionic conductivities than Selemion AMV. Prior work on chemistries similar to Selemion AMV suggest that the crosslinker content in Selemion is less than 20 wt. %.[18] Most of the membranes prepared in this study contained much higher amounts of crosslinker, which appears to limit both water content and ionic conductivity.

3.4 Optimizing poly(vinylimidazolium) anion exchange membranes for artificial photosynthesis

To optimize poly(vinylimidazolium) anion exchange membranes for artificial photosynthesis devices, the permeability of small CO_2 reduction products such as methanol should be minimized and the ionic conductivity must be adequate to support the current density of the photoelectrochemical device.[14,25,57,58] As shown in Section 3.2, the methanol permeability of all poly(vinylimidazolium) membranes had an exponential dependence on inverse water volume fraction. Furthermore, as shown in Section 3.3, the maximum ionic conductivity of poly(vinylimidazolium) membranes also appeared to correlate with inverse water volume fraction. These relationships suggest a tradeoff between CO_2 reduction product permeability and electrolyte ionic conductivity (Figure 10), where both of these properties are linked with membrane water content. For the materials described here, CO_2 reduction product permeability generally increases with increasing ionic conductivity for the membranes described in this study. For CO_2 reduction devices, the target membrane material will strongly depend on the device details such as required current density, geometry, and electrolyte conductivity. Membrane thickness can be used to control permeance and conductance, but material properties must be reasonable so that excessively thick or thin membranes are avoided. Thick membranes waste

expensive material, while thin membranes could be subject to mechanical failure and other degradation concerns.

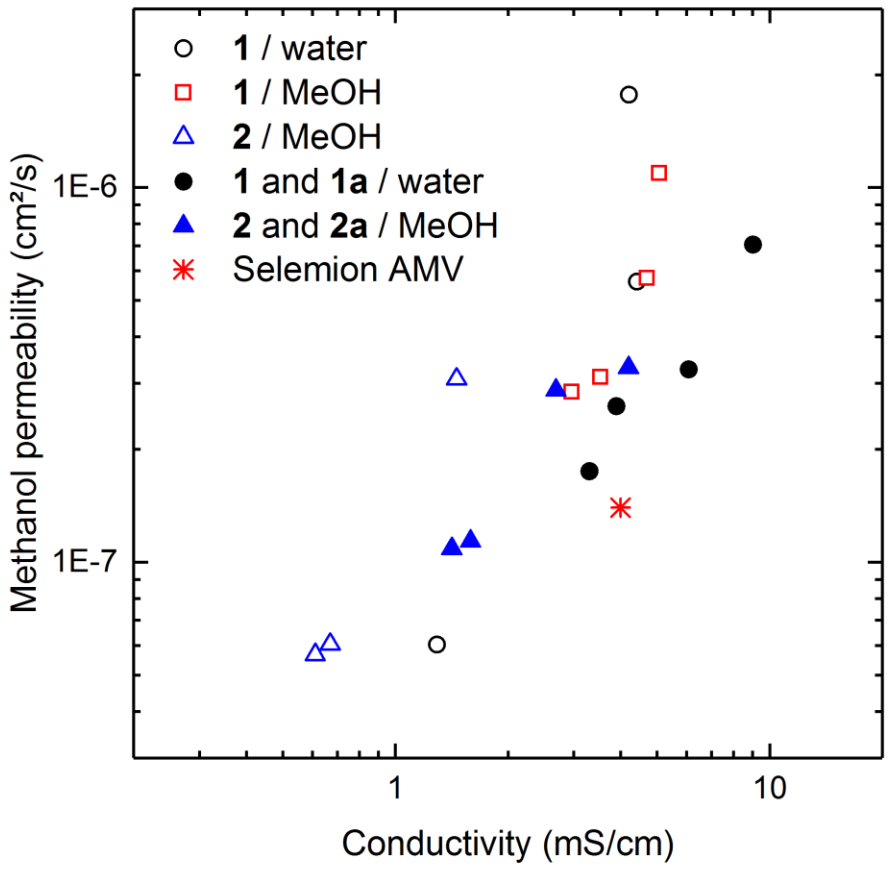

Figure 10. Tradeoff between methanol permeability and ionic conductivity for the membranes described in this study and commercial Selemion AMV. Generally, the most desirable membranes would appear in the lower right corner (high ionic conductivity and low CO_2 reduction product permeability).

Collectively, these poly(vinylimidazolium) materials offer a range of tunable permeabilities and ionic conductivities that could be suitable for photoelectrochemical CO_2

reduction devices. However, the absence of materials appearing in the lower right corner of Figure 10 and the correlation of water content with both methanol permeability and ionic conductivity highlight the material design challenges inherent to membrane development for CO_2 reduction devices.

4. Conclusions

A series of crosslinked poly(vinylimidazolium) anion exchange membranes were prepared with two different difunctional monomers with different alkyl spacer lengths. Monofunctional analogs of these monomers were incorporated to vary the crosslinker content but maintain a constant IEC. The prepolymerization solvent content was varied and the water uptake, methanol permeability, and ionic conductivity of the membranes were measured. Water content in the membranes increased with increasing prepolymerization solvent and/or monofunctional monomer content. As the length of the alkyl spacer was increased, equilibrium water content in the membranes decreased. Methanol permeability increased with increasing prepolymerization solvent content and increasing proportion of monofunctional monomer, both of which increased membrane water content. The methanol permeability of all prepared membranes was correlated to an exponential dependence on the inverse water volume fraction, which is consistent with free volume theory.[43,44] This result suggests that only changing the polymer structure may not be sufficient to limit small solute permeability, unless these changes result in a decrease in the water volume fraction of the membrane. Maximum ionic conductivities for poly(vinylimidazolium) membranes also appeared to correlate with inverse water volume fraction. Additional study is needed to better understand relationships between ionic conductivity, water volume fraction, and crosslink density. It is also important to understand how these anion exchange membranes

behave at higher solute concentrations and simultaneous measurements of the solute sorption characteristics could offer additional insights into structure-property relationships in anion exchange materials.

5. Conflicts of Interest

There are no conflicts to declare.

6. Acknowledgments

This material is based upon work performed at the Joint Center for Artificial Photosynthesis, a DOE Energy Innovation Hub, supported through the Office of Science of the U.S. Department of Energy under Award Number DE-SC000493. M.W. acknowledges the support through an Alexander-von-Humboldt Professorship. L.K. acknowledges financial support from the German Academic Exchange Service (DAAD) through its thematic network ACalNet (project #57267861). The authors thank Dr. Francesca Toma for helpful discussions.

6. References

1 G. M. Geise, D. R. Paul and B. D. Freeman, *Prog. Polym. Sci.*, 2013, **39**, 1–42.

2 J. Kamcev and B. D. Freeman, *Annu. Rev. Chem. Biomol. Eng.*, 2016, **7**, 111–133.

3 M. A. Hickner, A. M. Herring and E. B. Coughlin, *J. Polym. Sci. Part B Polym. Phys.*, 2013, **51**, 1727–1735.

4 M. Galizia, D. R. Paul and B. D. Freeman, *Polymer*, 2016, **102**, 281–291.

5 J. R. Varcoe, P. Atanassov, D. R. Dekel, A. M. Herring, M. a. Hickner, P. a. Kohl, A. R.

Kucernak, W. E. Mustain, K. Nijmeijer, K. Scott, T. Xu and L. Zhuang, *Energy Environ. Sci.*, 2014, **7**, 3135–3191.

6 N. Li, L. Wang and M. Hickner, *Chem. Commun.*, 2014, **50**, 4092–4095.

7 N. J. Robertson, H. A. Kostalik, T. J. Clark, P. F. Mutolo, H. D. Abruña and G. W. Coates, *J. Am. Chem. Soc.*, 2010, **132**, 3400–3404.

8 V. Neburchilov, J. Martin, H. Wang and J. Zhang, *J. Power Sources*, 2007, **169**, 221–238.

9 J. Michl, *Nat. Chem.*, 2011, **3**, 268–269.

10 J. A. Trainham, J. Newman, C. A. Bonino, P. G. Hoertz and N. Akunuri, *Curr. Opin. Chem. Eng.*, 2012, **1**, 204–210.

11 K. P. Kuhl, E. R. Cave, D. N. Abram and T. F. Jaramillo, *Energy Environ. Sci.*, 2012, **5**, 7050–7059.

12 E. L. Clark, M. R. Singh, Y. Kwon and A. T. Bell, *Anal. Chem.*, 2015, **87**, 8013–8020.

13 Gurudayal, J. Bullock, D. F. Srankó, C. M. Towle, Y. Lum, M. Hettick, M. C. Scott, A. Javey and J. Ager, *Energy Environ. Sci.*, 2017, **10**, 2222–2230.

14 M. R. Singh and A. T. Bell, *Energy Environ. Sci.*, 2016, **9**, 193–199.

15 Y.-G. Kim, A. Javier, J. H. Baricuatro and M. P. Soriaga, *Electrocatalysis*, 2016, **7**, 391–399.

16 M. R. Singh, E. L. Clark and A. T. Bell, *Phys. Chem. Chem. Phys.*, 2015, **17**, 18924–18936.

17 I. Merino-Garcia, E. Alvarez-Guerra, J. Albo and A. Irabien, *Chem. Eng. J.*, 2016, **305**,

104–120.

18 Y. Mizutani, R. Yamane, H. Ihara and H. Motomura, *Bull. Chem. Soc. Jpn.*, 1963, **36**, 361–366.

19 X. T. Le, T. H. Bui, P. Viel, T. Berthelot and S. Palacin, *J. Memb. Sci.*, 2009, **340**, 133–140.

20 G. A. Giffin, S. Lavina, G. Pace and V. Di Noto, *J. Phys. Chem. C*, 2012, **116**, 23965–23973.

21 E. L. Clark, C. Hahn, T. F. Jaramillo and A. T. Bell, *J. Am. Chem. Soc.*, 2017, **139**, 15848–15857.

22 Y. Lum, B. Yue, P. Lobaccaro, A. T. Bell and J. W. Ager, *J. Phys. Chem. C*, 2017, **121**, 14191–14203.

23 R. S. Kingsbury, S. Zhu, S. Flotron and O. Coronell, *ACS Appl. Mater. Interfaces*, 2018, **10**, 39745–39756.

24 R. B. Kutz, Q. Chen, H. Yang, S. D. Sajjad, Z. Liu and I. R. Masel, *Energy Technol.*, 2017, **5**, 929–936.

25 H. Yang, J. J. Kaczur, S. D. Sajjad and R. I. Masel, *J. CO2 Util.*, 2017, **20**, 208–217.

26 J. J. Kaczur, H. Yang, Z. Liu, S. D. Sajjad and R. I. Masel, *Front. Chem.*, 2018, **6**, 1–16.

27 J. Cui, N. Gao, J. Li, C. Wang, H. Wang, M. Zhou, M. Zhang and G. Li, *J. Mater. Chem. C*, 2015, **3**, 623–631.

28 T. K. Carlisle, G. D. Nicodemus, D. L. Gin and R. D. Noble, *J. Memb. Sci.*, 2012, **397**–

398, 24–37.

29 J. L. Anderson and D. W. Armstrong, *Anal. Chem.*, 2005, **77**, 6453–6462.

30 O. Nacham, K. D. Clark and J. L. Anderson, *Anal. Chem.*, 2016, **88**, 7813–7820.

31 Z. Zheng, Q. Xu, J. Guo, J. Qin, H. Mao, B. Wang and F. Yan, *ACS Appl. Mater. Interfaces*, 2016, **8**, 12684–12692.

32 Y. Yang, N. Sun, P. Sun and L. Zheng, *RSC Adv.*, 2016, **6**, 25311–25318.

33 B. M. Carter, B. M. Dobyns, B. S. Beckingham and D. J. Miller, *Polymer*, 2017, **123**, 144–152.

34 B. S. Beckingham, N. A. Lynd and D. J. Miller, *J. Memb. Sci.*, 2018, **550**, 348–356.

35 L. A. Robertson and D. L. Gin, *ACS Macro Lett.*, 2016, **5**, 844–848.

36 W. L. Hinze, B. Moreno, F. H. Quina, Y. Suzuki and H. Wang, *Anal. Chem.*, 1994, **66**, 3449–3457.

37 T. D. Ho, H. Yu, W. T. S. Cole and J. L. Anderson, *Anal. Chem.*, 2012, **84**, 9520–9528.

38 H. Yasuda, C. E. Lamaze and L. D. Ikenberry, *Makromol. Chemie*, 1968, **118**, 19–35.

39 H. Ju, B. D. McCloskey, A. C. Sagle, Y.-H. Wu, V. A. Kusuma and B. D. Freeman, *J. Memb. Sci.*, 2008, **307**, 260–267.

40 G. M. Geise, C. L. Willis, C. M. Doherty, A. J. Hill, T. J. Bastow, J. Ford, K. I. Winey, B. D. Freeman and D. R. Paul, *Ind. Eng. Chem. Res.*, 2013, **52**, 1056–1068.

41 G. M. Geise, M. A. Hickner and B. E. Logan, *ACS Appl. Mater. Interfaces*, 2013, **5**, 10294–301.

42 K. R. Cooper, *ECS Trans.*, 2011, **41**, 1371–1380.

43 L. Masaro and X. X. Zhu, *Physical models of diffusion for polymer solutions, gels and solids*, 1999, vol. 24.

44 H. Yasuda, L. D. Ikenberry and C. E. Lamaze, *Makromol. Chemie*, 1969, **125**, 108–118.

45 H. Ju, A. C. Sagle, B. D. Freeman, J. I. Mardel and A. J. Hill, *J. Memb. Sci.*, 2010, **358**, 131–141.

46 K. Dušek, *J. Polym. Sci. Part C Polym. Symp.*, 1967, **16**, 1289–1299.

47 Q. Tran-Cong-Miyata and H. Nakanishi, *Polym. Int.*, 2017, **66**, 213–222.

48 J. B. Greenblatt, D. J. Miller, J. W. Ager, F. A. Houle and I. D. Sharp, *Joule*, 2018, **2**, 381–420.

49 I. Ganesh, *Renew. Sustain. Energy Rev.*, 2014, **31**, 221–257.

50 X. Ren, T. E. Springer and S. Gottesfeld, *J. Electrochem. Soc.*, 2000, **147**, 92.

51 S. Mondal, S. Soam and P. P. Kundu, *J. Memb. Sci.*, 2015, **474**, 140–147.

52 Y. S. Kim, M. J. Sumner, W. L. Harrison, J. S. Riffle, J. E. McGrath and B. S. Pivovar, *J. Electrochem. Soc.*, 2004, **151**, A2150–A2156.

53 J. G. Wijmans and R. W. Baker, *J. Memb. Sci.*, 1995, **107**, 1–21.

54 J. Yan and M. A. Hickner, *Macromolecules*, 2010, **43**, 2349–2356.

55 G. Merle, M. Wessling and K. Nijmeijer, *J. Memb. Sci.*, 2011, **377**, 1–35.

56 L. M. Robeson, H. H. Hwu and J. E. McGrath, *J. Memb. Sci.*, 2007, **302**, 70–77.

57 A. Berger, R. A. Segalman and J. Newman, *Energy Environ. Sci.*, 2014, **7**, 1468–1476.

58 Y. Chen, N. S. Lewis and C. Xiang, *Energy Environ. Sci.*, 2015, **8**, 3663–3674.